



# Performance of graphene oxide as a water-repellent coating nanomaterial to extend the service life of concrete structures

Andrea Antolín-Rodríguez<sup>a,\*</sup>, Daniel Merino-Maldonado<sup>a</sup>, José M. González-Domínguez<sup>b</sup>, María Fernández-Raga<sup>c</sup>, Julia M<sup>a</sup>. Morán-del Pozo<sup>a</sup>, Julia García-González<sup>a</sup>, Andrés Juan-Valdés<sup>a</sup>

<sup>a</sup> INMATECO, Department of Agricultural Engineering and Sciences, School of Agricultural and Forest Engineering, University of Leon, Spain

<sup>b</sup> Instituto de Carboquímica (ICB-CSIC), Group of Carbon Nanostructures and Nanotechnology (G-CNN), C/Miguel Luesma Castán 4, 50018 Zaragoza, Spain

<sup>c</sup> Department of Chemistry and Applied Physics, Industrial Engineering School, University of Leon, Vegazana Campus S/N, 24071 Leon, Spain

## ARTICLE INFO

### Keywords:

Cement-based material  
Graphene oxide  
Coating  
Durability

## ABSTRACT

Surface treatments help to protect the built heritage against damage (environmental, accidental, etc.), reducing repair and restitution costs and increasing the useful life of building materials. The use of nanomaterials is currently the most important field of research in surface treatment technology for the preservation of building materials and, more specifically, to improve their durability and prevent their deterioration, extending their useful life. This paper studies the influence of a graphene oxide (GO) suspension as a surface treatment on the properties of concrete. The results indicate that, at best, surface treatment with GO can decrease both the water absorption and capillary absorption of concrete by about 15 %. The increase in the amount of GO deposited as a surface treatment leads to a further reduction in concrete water absorption. It is shown that, at best, GO coating also reduces water penetration at low and high pressures by approximately 20 % and 60 %, respectively. In addition, scanning electron microscopy analysis shows that GO surface treatment facilitates the hydration process and densifies the concrete microstructure. A simple aqueous suspension of GO is revealed as a tool with a high potential to protect concrete surfaces in a fast and cost-effective way, thanks to the easy application by spraying and the small amount of material needed to obtain great results.

## 1. Introduction

The worldwide demand for buildings and infrastructure is extremely high, with concrete being the most widely used material in modern and contemporary construction [1]. Concrete structures are exposed to different environmental conditions (cold, heat, rain) that lead to their erosion. Consequently, they are expected to exhibit high quality and durability properties to withstand these conditions during their design life [2]. Despite this perspective, several studies [3,4] have shown that, due to the microcracks and permeability of concrete, environmental liquids and gases are able to penetrate into the material, which can directly or indirectly cause its degradation and deterioration, shortening its service life.

Construction is one of the factors that has the greatest impact on the environment. The materials required for the development of

\* Corresponding author.

E-mail address: [aantr@unileon.es](mailto:aantr@unileon.es) (A. Antolín-Rodríguez).

<https://doi.org/10.1016/j.heliyon.2023.e23969>

Received 28 September 2023; Received in revised form 22 December 2023; Accepted 28 December 2023

Available online 29 December 2023

2405-8440/© 2024 The Authors. Published by Elsevier Ltd. This is an open access article under the CC BY-NC-ND license (<http://creativecommons.org/licenses/by-nc-nd/4.0/>).

this activity cause a large consumption of natural resources, which has led to great environmental pressure [5]. In addition, this activity also causes the problem of the generation of construction and demolition waste (CDW). This type of waste produced is the largest contributor to the waste generation flow [6]. Thus, the main challenges facing the conservation of construction materials are born. All of them committed to the promotion of environmentally sustainable construction, implementing new innovative practices to reduce the environmental impact [7]. According to data from the World Cement and Concrete Association [8], concrete consumption is estimated at 14 billion  $\text{m}^3 \text{ year}^{-1}$ , which represents approximately 35,109 tons  $\text{year}^{-1}$ , making it by far the most used artificial material by mankind. Therefore, any technique that allows increasing the useful life of this material will indirectly achieve a considerable improvement in sustainability, by reducing the use of raw materials (sands and gravels) and the use of cement or other binders, also achieving a significant reduction in energy consumption (it is estimated that between 3 % and 4 % of global energy consumption is associated with the production of concrete [9] and a reduction of  $\text{CO}_2$  emissions, of which 8 % are linked to the industry of this material [10]).

In addition, as a positive effect of the increase in its useful life, the natural carbonation processes of concrete tend to absorb a significant amount of atmospheric  $\text{CO}_2$  [8], so that treatments aimed at maintaining this material in service conditions during its useful life will reduce the impact of greenhouse gases (GHGs) on the living conditions of our planet, also significantly reducing the carbon footprint and mitigating the effects of climate change.

In the construction field, during the last decades the great concern for the deterioration of reinforced concrete structures has highlighted the need to intervene to ensure their preservation [11]. The most commonly adopted strategy is the use of high-performance concretes characterized by high strength and low permeability. However, more economical approaches against degradation are being studied to provide additional protection to the materials [12,13], such as: the use of low water/cement (w/c) ratios, the use of corrosion inhibitors or cathodic protection systems, or the treatment of concrete surfaces [14,15]. The use of new synthetic materials known as metamaterials or intelligent materials is a promising line of study and research that opens up new avenues of work at different levels and satisfactorily addresses some of the most important challenges that human beings will have to face in the coming decades. Among them, nanomaterials stand out, with different applications in various fields of work: treatment of wastewater, catalysis construction, biomedical engineering, energy, etc. [16–19]. The most widely accepted approach is the treatment of concrete surfaces due to its effectiveness in preventing and protecting against the entry of aggressive substances, avoiding the loss of durability of concrete structures or extending their lifespan [20]. In this regard, hydrophobic materials and those that act as a physical barrier to the penetration of ions, water and gases stand out as surface protection materials [21–23].

Recently, the search for strategies to improve the performance of traditional coatings and the durability of constructions has played an important role in the emergence of nanomaterials [24,25]. The use of nanocomposite coatings for surface treatment has attracted increasing interest among researchers because of their extraordinary potential to penetrate through the pores and cracks of concrete and heal damage [26]. There are numerous works related to the use of some nanoparticles, such as,  $\text{TiO}_2$ ,  $\text{SiO}_2$ ,  $\text{Al}_2\text{O}_3$ ,  $\text{ZnO}_2$ ,  $\text{CuO}$ ,  $\text{Fe}_2\text{O}_3$ ,  $\text{CaCO}_3$  that increase the quality of cementitious components, improving the mechanical, microstructural and durability properties of concrete [27,28]. However, so far most of the literature has focused on the study of these nanoparticles as an additive to the concrete mixture, with few studies on other techniques such as the use of these materials as surface treatments. Leung et al. [29] found that surface treatment of concrete with nanosilane-clay exhibited impermeable properties and improved resistance against chloride ions ingress, because the treatment is able to modify the microstructure of the concrete surface. At the same time, nano- $\text{SiO}_2$  surface treatments are compatible with the cementitious base [30] and increase concrete performance by blocking capillary pores against chloride ions penetration [11,31,32].

Considering that the current lines of research are focused on the search for new surface treatments based on nanomaterials, this study proposes the use of GO as a nanomaterial for the protection of concrete. In addition, this line of research is pursued since there are several studies that opt to include GO nanoparticles as an additive in the concrete mix, however there are current studies that express a problem of flocculation of nanoparticles in the presence of  $\text{Ca}^{+2}$  when they are added as an additive to the concrete mix [33, 34]. This problem, together with the high cost of nanoparticles compared to the rest of the concrete components, have led this study to focus on the use of nanomaterials as a surface treatment. And the GO nanosheets have been recognized as a very effective protective agent for carbonated stones [35], similarly process may occur on concrete. In the study conducted, graphene-based nanostructures have been used as potential agents to develop a protective treatment for concrete structures. Nanomaterials obtained from graphite, in this case graphene oxide, possess superior properties comparable to those of the nanomaterials such as nano- $\text{Al}_2\text{O}_3$ , nano- $\text{SiO}_2$ , nano- $\text{TiO}_2$  [36]. In addition, graphene-based particles have already been used as carbon nanofillers for the other types of hosting matrices, such as epoxy resins. These nanoparticles have been able to provide additional functional performance, including reduced sorption value in liquid water equilibrium and increased performance in mechanical properties, thanks to the particular arrangements of the graphene sheets [37].

Graphene oxide (GO) belongs to the graphene family of nanomaterials and is one of the most hydrophilic relatives, as it has a huge and diverse amount of oxygen functional groups [38], which enables the formation of stable single-sheet GO colloids by easy exfoliation of graphite oxide in water. GO has a favorable set of mechanical properties [39]. The diluted aqueous suspension of GO may look somewhat dark, but after application on concrete surfaces there is no color variation. Moreover, GO is industrially-produced in large amounts, thus available at competitive prices [40]. Based on the aforementioned properties and published studies [41,42], the application of GO could be a suitable strategy to protect concrete structures. In this work, the controlled application of aqueous GO coatings on hardened concrete samples is performed, demonstrating the remarkable protective efficacy of the treatment by improving the water uptake resistance and reducing the permeability of the concrete, without the need of any other adjuvant.

## 2. Experimental section

### 2.1. Materials

#### 2.1.1. Conventional concrete

Blast-furnace slag cement type CEM III/A 42.5 N/SR was used to mix conventional concrete, which complies with the standards of the European standard EN 197-1 [43], its chemical composition is specified in Table 1.

Natural siliceous gravel (4/12.5 mm) was used as coarse aggregate and natural siliceous sand (0/4 mm) as fine aggregate. The aggregates used have been characterized in accordance with standard EN 12620:2003+A1 [44]. The particle size distribution of the aggregates is determined according to standard EN 933-1 [45] and is shown in Fig. 1, which shows on the x-axis the size of the different sieves used and, on the y-axis, the % of the mass passing through each of them. Table 2 shows the proportion of the concrete mix used, specifying the amount of the components that make up the mix.

The water/cement ratio (W/C) was adopted based on the expected exposure of the concrete, in this case XC, considered an exposure to carbonation-induced corrosion. In addition, the dosage used complies with the durability standards for concrete structures of the Spanish Structural Code [46] which establishes a maximum w/c ratio of 0.60 and a minimum cement content of 200 kg m<sup>-3</sup> for type XC exposures.

#### 2.1.2. Graphene oxide

The GO used to coat cement-based samples in the present work was obtained through exfoliation of graphitic oxide in water upon the application of mild ultrasounds. In turn, such graphitic oxide was fabricated by the well-known Hummers oxidation method applied to graphite, with particular modifications. The whole experimental information is reported in full detail elsewhere [47], as well as a complete characterization of both graphitic oxide and GO.

An example transmission electron microscopy (TEM) image of freshly exfoliated GO is shown in Fig. 2, in which the thin and bidimensional nature of this material is evidenced, as well as its flexibility and physical adaptability (judged by its wrinkles and folds), reasserting it to be a very suitable asset at a microscopic level for a protective coating over many surfaces.

### 2.2. Methods

#### 2.2.1. Surface treatment of concrete

The concrete samples were coated with an aqueous suspension of GO without any other additives, with a concentration of 0.5 mg/ml. The application of the treatment was done by manual spraying with an airbrush, each coating pass was done with a horizontal movement at a slow and constant rhythm; always controlling the amount of GO suspension deposited on the sample. To evaluate the effect of GO as a surface coating of concrete against water penetration, two groups of coated samples were studied. The first group of samples (1-GO) has an amount of 10.5 µg cm<sup>-2</sup> of GO, and the second group of samples (3-GO) has an amount of 31.5 µg cm<sup>-2</sup> of GO. Table 3 shows in detail the type of samples studied, the amount of dispersion used as surface treatment and the amount of GO deposited on the concrete sample.

Four different tests were performed to evaluate the water resistance of GO deposited on the concrete surface. Each test required the preparation of concrete samples with particular properties in terms of surface area, so four types of samples are classified according to this requirement. Table 4 shows in detail the type of test performed, the types of specimens required for each test (the number of specimens studied and their required dimensions) and the surface area tested. The concrete samples used were cured for 28 days prior to treatment.

#### 2.2.2. Durability tests

The focus of this study is to determine the efficacy and performance of GO as a protective coating for concrete surfaces to increase their water resistance. To this end, concrete samples with different concentrations of GO on the surface are compared with untreated concrete samples in a set of water absorption and surface porosity tests. The tests are specified below.

**2.2.2.1. Determination of water absorption by capillary action.** The capillary water absorption test has been developed to evaluate the permeability of concrete. Almost all water penetration into concrete occurs mainly by capillary absorption force, which is provided by

**Table 1**  
Chemical composition of cement.

Chemical composition	Value (wt. %)
Al <sub>2</sub> O <sub>3</sub>	7.20
SiO <sub>2</sub>	25.00
Fe <sub>2</sub> O <sub>3</sub>	2.03
SO <sub>3</sub>	2.70
CaO	51.80
MgO	4.68
TiO <sub>2</sub>	0.60
Loss on Ignition	4.53

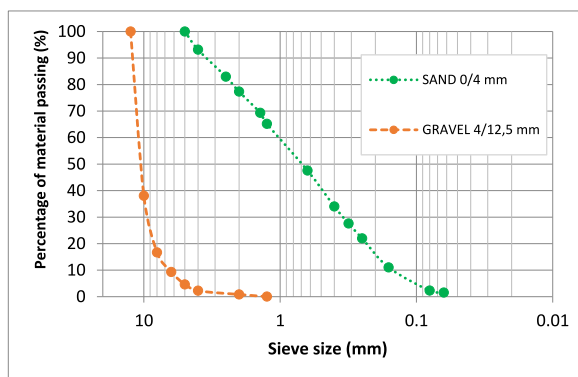


Fig. 1. Particle size distribution of natural aggregates (coarse and fine) used in the production of concrete.

Table 2

Mix proportion of concrete.

Mix proportion	Coarse Aggregate ( $\text{kg m}^{-3}$ )	Fine Aggregate ( $\text{kg m}^{-3}$ )	Cement ( $\text{kg m}^{-3}$ )	W/C
Conventional concrete	1030.71	650.49	390.00	0.51

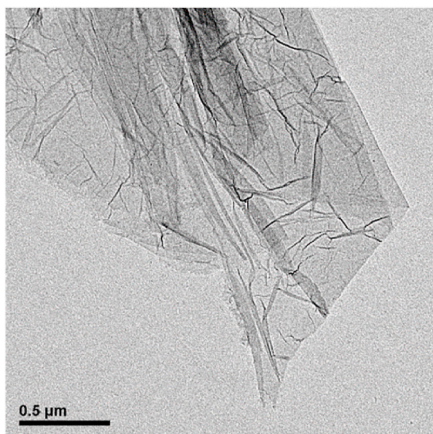


Fig. 2. TEM image of a GO flake. Recorded with a JEOL-200FXII microscope working at 200 kV and with 0.28 nm point-to-point resolution. Sample deposited over a 400-mesh copper grids (Electron Microscopy Sciences, ref CF-400CU).

Table 3

Details of surface treatment applied.

Samples groups	Amount of dispersion ( $\text{mg cm}^{-2}$ )	GO content ( $\mu\text{g cm}^{-2}$ )
Control (uncoated)	0.0	0.0
1-GO	21.0	10.5
3-GO	63.0	31.5

pore absorption and surface tension [48]. During this water penetration process, aggressive ions enter the concrete, so capillary water absorption is a critical parameter of concrete durability to be studied [49].

To evaluate the capillary water absorption of the concrete samples, the permeability test is performed according to standard EN 83982 [50]. Previously, samples are conditioned in accordance with EN 83966 [51]. To ensure that water absorption occurs only on the treated surface, the other faces of the specimen in contact with the water are sealed with a layer of paraffin approximately 1 cm high.

The specimens are placed in a plastic container with a leveling grid, on which the specimens were placed in contact with deionized water about 5 mm in height. After set periods of time (5 min, 10 min, 15 min, 30 min, 1 h, 2 h, 3 h, 4 h, 6 h, 24 h, 48 h, 96 h, until the mass is constant), surface water is removed from the samples with a damp cloth and tested samples are weighed.

**Table 4**  
Types of samples and tests.

Test methods	Sample specimens		Test surface (cm <sup>2</sup> )
	Amount	Dimensions (cm)	
Capillary water absorption	4	10 x 10 x 10	10*10
Water absorption by immersion	4	10 x 10 x 10	600.0
Karsten tubes	2	10 x 10 x 40	10*40
Water absorption under pressure	4	Ø10 x 20	π*5 <sup>2</sup>
SEM	4	Ø2.5 x 1	π*1.25 <sup>2</sup>

To further investigate the effectiveness of the surface treatment used, the capillary water absorption coefficient (K) is calculated for each of the samples, using Equation (1) established in EN 83982 [50]:

$$K = \frac{\delta_a \cdot \varepsilon_e}{10 \cdot \sqrt{m}} \quad (1)$$

Where K is the capillary absorption coefficient (kg m<sup>-2</sup> min<sup>-0.5</sup>),  $\delta_a$  is the density of water (the value of 1 g cm<sup>-3</sup> is considered),  $\varepsilon_e$  is the effective porosity of concrete (cm<sup>3</sup> cm<sup>-3</sup>) and m is the resistance to water penetration by capillary absorption (min cm<sup>-2</sup>).

**2.2.2.2. Determination of water absorption by immersion.** The method used to determine the water absorption of concrete is described in the standard EN 83980 [52]. The objective of this test was to determine the volumetric absorption of the treated concrete as an indicator of the important role of the protective surface agents, for this purpose the surface treatment is applied on all the faces of the specimens. The mass of the specimens was recorded every 24 h, until constant mass. Equation (2) was used to calculate the volumetric absorption of the different concrete samples:

$$WA (\%) = \frac{w_t - w_o}{w_o} \cdot 100 \quad (2)$$

Where  $w_o$  is the mass of the oven-dried concrete specimen (g) and  $w_t$  is the mass of the concrete specimen after immersion in water (g).

**2.2.2.3. Water absorption at low pressure (Karsten tubes).** This method is often used to quantify water permeability at low pressures and to define the degree of protection and effectiveness provided by surface treatments over a given period of time, since the water pressures used simulate the effect of rain on the concrete surface [53].

The test protocol is described in EN 16302 [54]. The test uses so-called “Karsten tubes”, which are glass tubes graduated in tenths of millimeter, which are assembled to the concrete surface with butyl adhesive. The Karsten tubes are distributed homogeneously over the concrete surface to be studied, with a total of 6 data collection points per sample.

Once the tubes are in place, each tube is filled to the zero mark with distilled water. Subsequently, the time it takes for the water level to drop by 1 ml, meaning for the concrete absorbs 1 ml of water, is noted.

**2.2.2.4. Water penetration depth under pressure.** The test to determine the depth of water penetration under pressure for concrete was performed in accordance with EN 12390-8 [55]. The test is performed in water penetration equipment, in which the test surfaces are subjected to a hydrostatic pressure of 5 bar (0.5 MPa) for a period of 72 h.

The specimens are then removed from the test rig and subjected to indirect tensile stress so that they fracture perpendicular to the test surface. In this way it is possible to examine the depth of water penetration. This procedure was performed in accordance with EN 12390-6 [56].

After splitting the test specimen, the penetration profile is marked and the maximum penetration depth “ $P_{max}$ ” is recorded. In addition, the average depth of penetration is calculated according to Equation (3):

$$P_m = A_{pf} / d \quad (3)$$

Where  $P_m$  is the mean depth of penetration (mm), d is the sample diameter (mm) and  $A_{pf}$  is the area of the penetration front (mm<sup>2</sup>). A computer program (ImageJ) [57] was used to calculate the area of the penetration front.

### 2.2.3. Microscopic observations and spectra analysis

The surfaces of the concrete samples were subjected to microscopic visualization to acquire information on existing pores and microcracks and surface roughness. In addition, a quantitative chemical characterization of the surface of the samples is performed from EDX spectra (Energy Dispersive X-ray analyser). The samples were observed using a Hitachi S-4800 microscope with a tungsten X-ray source, a Si/Li detector and a Bruker XFlash 5030 EDS analyzer. Prior to analysis, the samples were coated with gold.

### 2.2.4. Statistical analysis

The data resulting from the various tests were subjected to a statistical analysis, more specifically, to a one-way ANOVA by comparison of means. The durability parameters (capillary absorption, absorption by immersion, low pressure water and pressurized

water penetration) were taken as variable factors, and the type of surface treatment given to the samples was taken as a fixed factor. The difference ( $p \leq 0.05$ ) between the results were studied by comparison of means through the LSD (Least Significant Difference) post-hoc test.

### 3. Results and discussion

#### 3.1. Determination of water absorption by capillary action

The capillary water absorption process of hardened concrete is represented by the typical water absorption curve, which relates mass gain as a function of time (Fig. 3). The absorption process is characterized by an initial state in which water fills the sample through the capillary pores without reaching the top of the sample, and a second state in which water continues to fill the sample, but this time through that air pores [58–60].

The results indicated that the control (uncoated) samples absorbed water for a longer period of time compared to the GO samples. The control (uncoated) samples reached constant mass at 120 h ( $85 \text{ min}^{0.5}$ ), while the 1-GO and 3-GO samples, stabilized at 96 h ( $76 \text{ min}^{0.5}$ ) and  $72 \text{ h}$  ( $66 \text{ min}^{0.5}$ ), respectively. In addition, the control specimens absorb a greater total amount of water than the GO-coated specimens. In Fig. 3, it can be seen that the surface treatment with GO reduces the capillary water absorption capacity of the concrete by 20 % and 31 %, respectively, compared to the control concrete.

One of the probable mechanisms that explain the reduction of the water permeability of concrete is the creation of a dense layer of GO on the surface of the concrete. Thanks to the exfoliation of the GO in suspension [61,62], the surface treatment performed evenly distributed the GO sheets on the surface of the concrete, thus creating that dense layer. Previous studies have shown that the oxygen functional groups present in the GO films can react with  $\text{Ca}(\text{OH})_2$  or CSH of the concrete [63], causing the GO to adhere strongly to the surface thereof. The creation of this bond can significantly reduce the amount and size of microcracks and pores on the surface of the concrete, and therefore, could reduce the permeability to water, reducing the process of water absorption by capillarity.

The effectiveness of nanomaterials as waterproofing agents used in concrete surface protection can be supported by the values of the capillary water absorption coefficient (K) shown in Fig. 4. Considering the minimum requirements established in standard EN 1504-2 [64], the water permeability coefficient should not exceed  $1.29 \times 10^{-2} \text{ kg m}^{-2} \text{ min}^{-0.5}$ . As can be seen, the values obtained comply with such requirement, so the protection can be accepted as a surface treatment. The results achieved in the statistical analysis determine that samples 1-GO, and samples 3-GO presented significant differences with respect to the Control (uncoated) samples; since the “K” coefficient was significantly lower ( $F = 86.032$ ;  $gl = 2.6$ ;  $p \leq 0.001$ ), leading to a decrease of 11 % and 23 %, respectively. This shows that GO can seal the pores of concrete, which reduces its capillary water absorption.

The capillary absorption process is one of the main causes of liquid transport in cement-based materials due to their porous nature [65], which can lead to a problem in the use of this type of materials for construction, as they can not only transport water but also other types of corrosive materials that would cause damage to the concrete [66].

These results compare favorably with several investigations on protective treatments of concrete made from nanomaterials. For example, Akbar et al. [67] reported that spraying three types of treatments with 20 % nanoparticles (nanosilica, nanomontmorillonite and nanohalloysite) dispersed in deionized water and an addition of NaOH, a reduced capillary absorption by 59 %, 50 % and 46 % is observed, respectively, relative to untreated samples. The results obtained are approximately 70 % higher than those of the present study, but it must be considered that they use a concentration on the order of 400 times higher and that the base of the dispersion has NaOH as an additive, which increases the stability of the dispersion but might be damaging at long term.

More in line with the research present in this study are the various investigations performed on the application of GO as an additive to increase the performance of other agents used as surface treatments. Zhang et al. [68] demonstrated that concrete specimens coated with two passages of a silane emulsion were enhanced with the addition of GO at a dosage of  $300 \text{ g m}^{-2}$  each reduced capillary absorption, showing a waterproofing effect of 90 %. Hou et al. [69] reported that a 2-passage coating at a dosage of  $600 \text{ g m}^{-2}$  of a silane emulsion modified with GO was able to reduce capillary water absorption by 86.9 % compared to reference samples. These

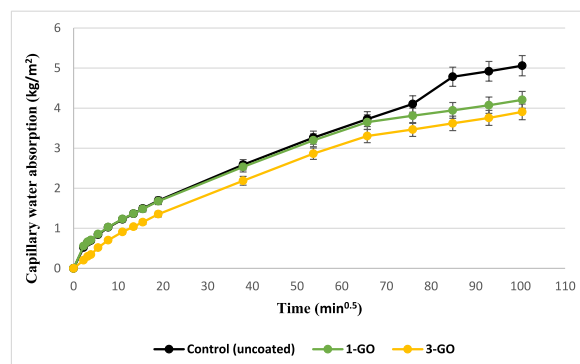
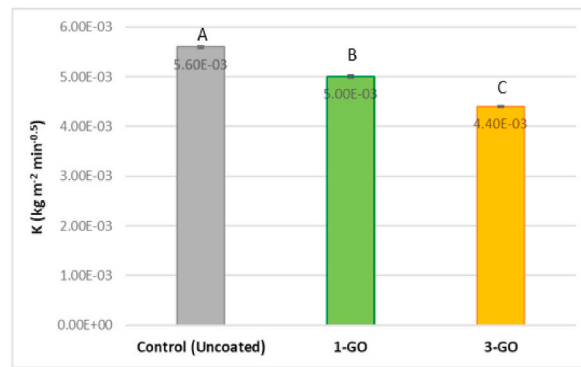


Fig. 3. Capillary water absorption in concrete specimens with GO surface treatment and without treatment.



**Fig. 4.** Capillary absorption coefficient values (K) for GO-coated and uncoated concrete specimens. Statistical differences in the results are marked with different capital letters (LSD test,  $p < 0.05$ ).

researchers achieve very good results with the coating used, but it is important to keep in mind that all these surface treatments are made up of several components necessary for the final effectiveness of the coating. The silane emulsion is able to penetrate the concrete and covalently bond to it, forming a hydrophobic silane layer within the concrete. The addition of GO increases the thickness of the hydrophobic layer and reduces the number of microscopic holes in the hydrophobic layer, thus improving the waterproofing effect.

### 3.2. Determination of water absorption by immersion

The durability properties of concrete are directly related to water absorption [70]. Fig. 5 shows the water absorption by immersion results obtained, which demonstrates the effectiveness of the surface treatment. After 24 h of immersion, the control (uncoated) samples show higher water absorption than the GO-coated samples. Thus, the control samples show a water absorption of approximately 4.3 %, while the coated samples show an absorption of 3.7 % and 2.5 %, for samples 1-GO and 3-GO, respectively. The water absorption of the 1-GO and 3-GO samples was significantly lower ( $F = 219.817$ ;  $gl = 2.6$ ;  $p \leq 0.001$ ) than that of the Control (uncoated) samples, decreasing water absorption by 15 % for the 1-GO samples and 42 % for the 3-GO samples. It is shown that increasing the GO content leads to a decrease in volumetric water absorption of concrete. This fact can be attributed to the creation of a protective layer on the concrete surface formed by uniformly distributed GO films [61]. These sheets interact physically and chemically with the CSH hydration products of the concrete [63], which can lead to the sealing of microcracks and pores, thus limiting volumetric water absorption. The results obtained are comparable to those obtained by Habibnejad Korayem et al. [41] who, after an immersion period of 24 h, were able to reduce water absorption by 40 % in concrete samples with the surface application of 16 mg of a GO dispersion (0.015 mg/ml) for 5 days, compared to uncoated control samples.

Despite studies on GO as a protective coating for concrete are very scarce, it is possible to establish comparison with other types of nanoparticles used as surface protectors of concrete. In such way Li et al. [71] demonstrated that the modification of organic resin coatings with nanoparticles (nano-SiO<sub>2</sub> and nano-TiO<sub>2</sub>) improved the hydrophobicity of concrete, reducing water absorption by 13.2 % nano-TiO<sub>2</sub> and 17.8 % for nano-SiO<sub>2</sub> modified coatings, relative to uncoated samples. As can be seen, these researchers achieved water absorption reduction values similar to those obtained with the surface application of three GO coating passages. It is important to note that the GO surface treatment is just a dispersion of GO in deionized water, whereas the one employed by these researchers is an organic resin with a nanoparticle dispersion and a silane coupling agent KH-570, which turns the coating into a much more complex system. In addition, they employ a 400-fold higher concentration of nanoparticles.

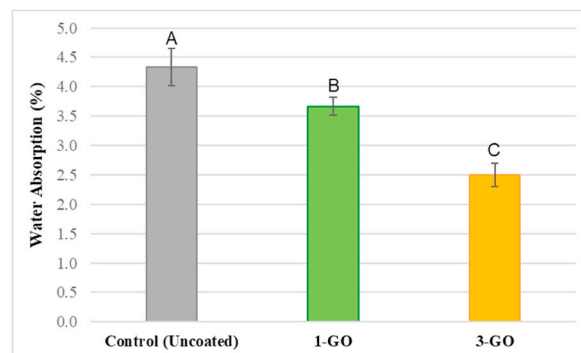


**Fig. 5.** Water absorption in uncoated and GO-coated concrete specimens. Statistical differences in the results are marked with different capital letters (LSD test,  $p < 0.05$ ).

### 3.3. Water absorption at low pressure (Karsten tubes)

Fig. 6 shows the results obtained for the different concrete samples subjected to the low-pressure water absorption test (Karsten tubes). The graph shows the amount of water absorbed by the concrete as a function of time, and the total time it took to absorb 1 ml of water can also be determined. When comparing the control (uncoated) and GO-coated samples, it can be seen that the time taken by the GO-coated samples is significantly longer, on the order of 15 % for the 1-GO samples and 20 % for the 3-GO samples, compared to the control samples. In addition, the results obtained for each of the Karsten tubes used in the test were similar, showing that the test surfaces were uniform.

In reference to Fig. 6, the readings taken during the test also provide the evolution of the absorption time for set values of water volume. It can be seen that both the initial rate (up to 0.1 ml) of water absorption for the control (uncoated) and GO-coated samples is similar. The absorption curve of samples 1-GO remains very similar to that of the control until 0.4 ml, where it begins to diverge, causing the absorption time of this samples to increase; just this moment coincides with the approach of this curve to the absorption curve of samples 3-GO. The absorption curve of sample 3-GO is the one with the longest absorption times.

The results obtained agree with the rest of the results obtained in the other test. In the control samples (uncoated), the pores and microcracks of the concrete are more accessible to water penetration, but when the GO coating is applied, they decrease, so that the application of the surface concentration of  $10.5 \mu\text{g cm}^{-2}$  GO forms a thin protective layer on the surface of the concrete, slightly decreasing the permeability to water [63,72]. Thus, if the surface concentration is increased to  $31.5 \mu\text{g cm}^{-2}$  GO, a thicker protective layer is produced, forming a preventive barrier against water ingress [41].

### 3.4. Water penetration depth under pressure

Fig. 7a show the maximum water penetration values ( $P_{\text{max}}$ ) reached in the different samples tested. The control samples (uncoated) recorded a  $P_{\text{max}} = 15.5$  mm. Thus, the samples 1-GO obtained a  $P_{\text{max}} = 10.9$  mm and the samples 3-GO obtained a  $P_{\text{max}} = 9.6$  mm. If the results obtained in the statistical analysis of the maximum water penetration ( $P_{\text{max}}$ ) are observed, it is determined that the samples with GO surface treatment presented significant differences with respect to the Control samples (uncoated), since the  $P_{\text{max}}$  was significantly lower ( $F = 36.138$ ;  $g1 = 2.6$ ;  $p \leq 0.001$ ) for the samples with GO than that obtained in the Control samples, decreasing by 30 % for the 1-GO samples and 38 % for the 3-GO samples.

In order to obtain a more representative study of the effectiveness of the coating, the mean value of the penetration depth ( $P_m$ ) is determined. Fig. 7b shows the  $P_m$  values for the various samples tested, such that the  $P_m$  value for the Control samples (uncoated) versus the samples coated with GO was significantly higher ( $F = 1590.250$ ;  $g1 = 2.6$ ;  $p \leq 0.001$ ), on the order of 43 % and 59 %, for samples 1-GO and 3-GO, respectively. These average depth values are more representative of coating effectiveness because water penetration in the tested samples is regular, such that water penetrates through the entire test surface (Fig. 8).

Observing the water penetration profile of the samples tested, it can be determined that they are different, since the application of GO on the surface of the concrete leads to the creation of a more uniform and homogeneous profile, with the 3-GO samples presenting the profile with the lowest penetration front. The creation of this type of profile may be due to the fact the spraying of the surface treatment uniformly distributes the GO sheets on the surface of the concrete, creating a dense layer that would increase the protective power [61,62]. In addition, protection against pressurized water penetration may be due to the fact that GO nanoparticles can act grains that, when adhering to the surface, cause disordered surface tropism due to the reduction of the size of  $\text{Ca}(\text{OH})_2$  crystal present in the concrete [73]. The creation of this interaction can significantly reduce the number and size of microcracks and pores on the concrete surface, creating a barrier to water penetration.

The results obtained compare favorably with several studies on surface treatments based on nanomaterials used for concrete protection. Among the most relevant studies is that of Ardalan et al. who managed to reduce the average water penetration under pressure by 31 % with respect to untreated samples, by spraying colloidal nano- $\text{SiO}_2$  oxide with a concentration of 12 %. Another relevant study is that of Akbar et al. by spraying three types of solutions containing 20 % nanoparticles (nanosilica, nanohalloysite and

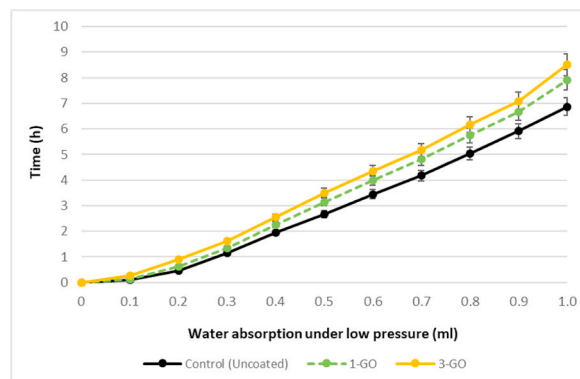


Fig. 6. Evolution of the absorption time in the low-pressure water absorption test.



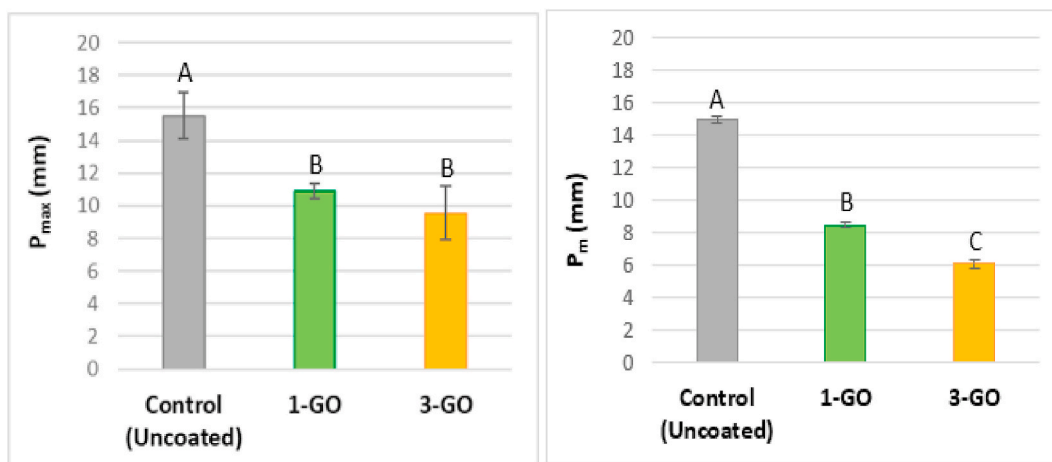


Fig. 7. Results of water penetration depth under pressure of uncoated and GO-coated concrete samples: (a) Maximum penetration depth " $P_{max}$ "; (b) Mean depth of penetration " $P_m$ ". Statistical differences in the results are marked with different capital letters (LSD test,  $p < 0.05$ ).

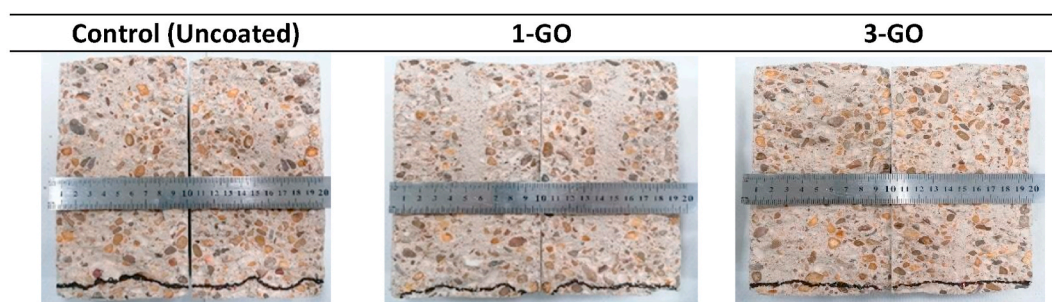


Fig. 8. Penetration profile after pressurized water test in concrete.

nanomontmorillonite) managed to reduce the water penetration depth by 48 %, 22 % and 30 % respectively, relative to the untreated samples. As can be seen, all these treatments achieve surface protection values against water penetration within the range of those obtained with the GO surface coating. However, these treatments are applied at a concentration about 400 times higher and have an addition of NaOH to increase their stability. For all these reasons, GO is presented as a treatment that offers better results, thanks to the fact that it does not require the incorporation on any stabilizing agent and the necessary concentration is much lower.

### 3.5. SEM and EDX analysis

Fig. 9 shows SEM micrographs and EDX spectra of a control concrete sample and two concrete samples with GO surface treatment, one with one GO coating passage (1-GO) and one with three GO coating passage (3-GO), which allow analysis of changes in surface morphology. The presence of the GO treatment on the surface of the concrete is confirmed by the EDX spectra of the samples, with strong peaks of oxygen, calcium and silicon, as there is a strong interaction between the oxygen functional groups present in the GO films with the hydration products of the CSH or  $\text{Ca}(\text{OH})_2$  [74]. The key to this fact is the assembly property of 2D graphene oxide [75]. Metal ions ( $\text{Al}^{3+}$ ,  $\text{Fe}^{3+}$ ,  $\text{La}^{3+}$ ,  $\text{Ca}^{3+}$ ,  $\text{Mg}^{2+}$ ,  $\text{Ni}^{2+}$ , etc.) have been found to act as crosslinking agents for GO membranes, these alkaline earth cations being some of the main components of the cement used for concrete production, so it is possible for GO to bond strongly to the surface by chemical bonding [76].

In relation to the micrographs, Fig. 9a show a concrete surface in which there is no treatment cover; it shows that there are microcracks and pores of different sizes in the hydration products of the concrete, all of them accessible to any type of substance. On the other hand, Fig. 9b and c shows the GO deposited on the concrete sample. The hydration products of these samples show fewer microcracks and smaller pore size compared to the control sample.

Comparing Fig. 9b and c, it is observed that the number and size of microcracks and pores in the hydration products are significantly reduced with increasing GO coating passages. In Fig. 9b, a thin coating layer has been created on the surface of the concrete, being sparse. However, Fig. 9c presents a denser coating layer on its surface, with the hydration products being completely covered and protected. As discussed by He et al. [77], the protective GO coating as the one studied in this research interacts with the microstructure of the concrete surface, decreasing the interconnectivity between the surface pores resulting in a barrier to the penetration of any kind of substance. Thus, the pore sealing ability of GO is certainly the explanation for the improvements in water resistance observed in the

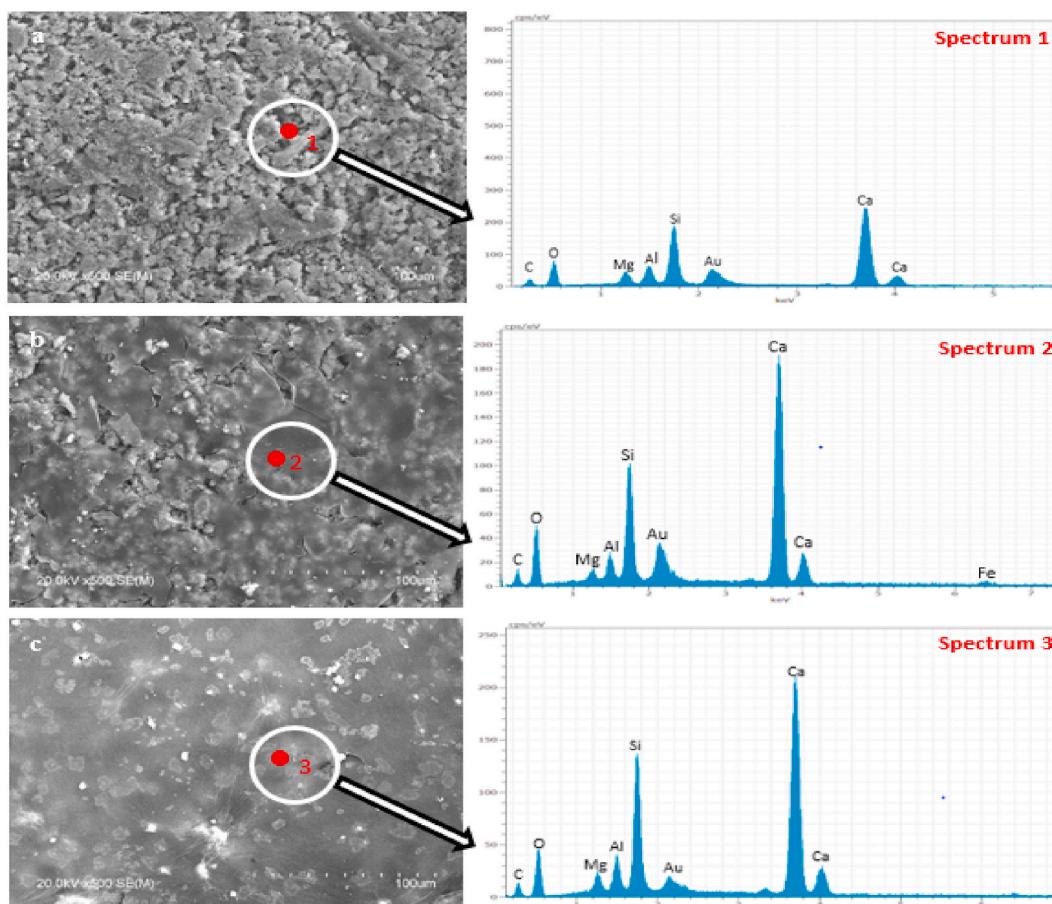


**Fig. 9.** SEM images showing surface microstructures and EDX spectra to show elemental compositions: (a) Control sample (uncoated); (b) 1-GO sample; (c) 3-GO sample.

results.

#### 4. Conclusions

This work investigated the suitability and potential of graphene oxide (GO) as a new protective surface coating material for concrete. Water transmission was analysed in concrete samples surface coated with and without GO. The following conclusions are drawn from the results obtained.

- According to the durability tests performed, GO performs strikingly well as a protective coating for concrete surfaces.
- The GO-coated concrete specimens improve over the reference specimens in all tests. It was shown that, at best, GO coating on the concrete surface reduces volumetric water absorption and capillary absorption by approximately 42 % and 23 %, respectively.
- The GO surface treatment was also effective against low pressure water absorption, showing at best an improvement of concrete impermeability by approximately 20 %.
- The highest effectiveness of the treatment occurs in the pressurized water penetration test, reaching almost 60 % of concrete impermeability for specimens with three GO coating passages ( $31.5 \mu\text{g cm}^{-2}$ ). In addition, this test confirmed the uniform distribution of the treatment over the concrete surfaces.
- The increasing in the surface concentration of the coating results in a progressive increase in surface impermeability due to the creation of a thicker protective layer on the concrete surface.
- The images show how the GO treatment remains on the external face of the concrete exerting the pore sealing effect but without penetrating into the interior, so that the application of the nanomaterial improves durability without affecting the internal microstructure of the concrete.

In light of the promising results obtained in the present study, spraying an aqueous colloidal suspension of GO without additives on concrete surfaces opens a new venue for study, as GO proves to be a durable coating and an immensely protective tool for preserving

concrete structures. In a real-world scenario, the concrete structures suffer deterioration mainly for the presence of water (the famous sentence “no water no problem” cited in numerous bibliographies resumes this problem). Water is the mainly entrance vehicle for aggressive agents which can damage concrete structures. The application of GO coatings in concrete can surely get to improve preservation of real structures, through diminishing water entrance in this material. More studies are necessary but, in a practical way, it can imply a reduction of cover thickness in reinforced concrete and/or an increasing of the life span. Studies such as the one presented in this document will serve to establish these real improvements in the near future.

Future lines of research will focus their efforts on the study of new dispersion concentrations used for surface treatment, with the aim of determining an optimum amount of treatment, as well as the study of new forms of application of this, being able to determine from the economic point of view which would be more appropriate.

### Data availability statement

The data have not deposited in a publicly accessible repository. Data supporting the results presented in this article are available from the corresponding author upon reasonable request.

### CRediT authorship contribution statement

**Andrea Antolín-Rodríguez:** Writing – review & editing, Writing – original draft, Software, Methodology, Investigation, Formal analysis, Data curation. **Daniel Merino-Maldonado:** Methodology, Investigation, Data curation. **José M. González-Domínguez:** Writing – review & editing, Writing – original draft, Resources, Formal analysis. **María Fernández-Raga:** Writing – review & editing, Resources, Formal analysis. **Julia García-González:** Writing – review & editing, Resources, Formal analysis. **Andrés Juan-Valdés:** Writing – review & editing, Writing – original draft, Supervision, Formal analysis.

### Declaration of competing interest

The authors declare that they have no known competing financial interests or personal relationships that could have appeared to influence the work reported in this paper.

### Acknowledgements

This work was supported by the Junta de Castilla y León through the “Ayudas para financiar la contratación predoctoral de personal investigador”, cofinanced by the European Social Fund and resulting in ORDEN EDU/875/2021 and ORDEN EDU/601/2020.

José Miguel González-Domínguez and María Fernández-Raga greatly acknowledge the Spanish Ministry of Science and Innovation (MICINN) for the funded project “Nanoshield” (PID2020-120439RA-I00)

### References

- [1] Y.A. Villagrán-Zaccardi, A.T.M. Marsh, M.E. Sosa, C.J. Zega, N. De Belie, S.A. Bernal, Complete re-utilization of waste concretes–Valorisation pathways and research needs, *Resour. Conserv. Recycl.* 177 (2022), <https://doi.org/10.1016/j.resconrec.2021.105955>.
- [2] X. Pan, Z. Shi, C. Shi, T.C. Ling, N. Li, A review on concrete surface treatment Part I: types and mechanisms, *Constr Build Mater* 132 (2017) 578–590, <https://doi.org/10.1016/j.conbuildmat.2016.12.025>.
- [3] C.S.S. Durga, N. Ruben, Assessment of various self healing materials to enhance the durability of concrete structures, *Ann. Chimie Sci. Matériaux* 43 (2019) 75–79, <https://doi.org/10.18280/acsm.430202>.
- [4] M. Liang, K. Feng, C. He, Y. Li, L. An, W. Guo, A meso-scale model toward concrete water permeability regarding aggregate permeability, *Constr Build Mater* 261 (2020), 120547, <https://doi.org/10.1016/j.conbuildmat.2020.120547>.
- [5] A. Juan-Valdés, D. Rodríguez-Robles, J. García-González, M.I. Sánchez de Rojas Gómez, M. Ignacio Guerra-Romero, N. De Belie, J.M. Morán-del Pozo, Mechanical and microstructural properties of recycled concretes mixed with ceramic recycled cement and secondary recycled aggregates. A viable option for future concrete, *Constr Build Mater* 270 (2021), <https://doi.org/10.1016/j.conbuildmat.2020.121455>.
- [6] S. Prakash, M. Wijayasundara, P.N. Pathirana, K. Law, De-risking resource recovery value chains for a circular economy – accounting for supply and demand variations in recycled aggregate concrete, *Resour. Conserv. Recycl.* 168 (2021), 105312, <https://doi.org/10.1016/j.resconrec.2020.105312>.
- [7] X. He, Z. Zheng, M. Ma, Y. Su, J. Yang, H. Tan, Y. Wang, B. Strnad, New treatment technology: the use of wet-milling concrete slurry waste to substitute cement, *J. Clean. Prod.* 242 (2020), 118347, <https://doi.org/10.1016/j.jclepro.2019.118347>.
- [8] Global Cement, Concrete Association, Concrete Future Roadmap Overview-Spanish, 2022.
- [9] A.M. Omer, Energy Efficiency Improvement Utilising High Technology: an Assessment of Energy Use in Industry, Buildings Development and Environment, 1995. <https://ssrn.com/abstract=2403145>.
- [10] R.J.A.G.M. T.A. Boden, Global, Regional, and National Fossil-Fuel CO<sub>2</sub> Emissions, Carbon Dioxide Information Analysis Center, Environmental System Science Data Infrastructure for a Virtual Ecosystem (ESS-DIVE) (United States), 2017.
- [11] E. Franzoni, B. Pigino, C. Pistolesi, Ethyl silicate for surface protection of concrete: performance in comparison with other inorganic surface treatments, *Cem. Concr. Compos.* 44 (2013) 69–76, <https://doi.org/10.1016/j.cemconcomp.2013.05.008>.
- [12] A.A. Almusallam, F.M. Khan, S.U. Dulaijan, O.S.B. Al-Amoudi, Effectiveness of surface coatings in improving concrete durability, *Cem. Concr. Compos.* 25 (2003) 473–481, [https://doi.org/10.1016/S0958-9465\(02\)00087-2](https://doi.org/10.1016/S0958-9465(02)00087-2).
- [13] F. Tittarelli, G. Moriconi, Comparison between surface and bulk hydrophobic treatment against corrosion of galvanized reinforcing steel in concrete, *Cem Concr Res* 41 (2011) 609–614, <https://doi.org/10.1016/j.cemconres.2011.03.011>.
- [14] R.B. Polder, W.H. A Peelen, B.J. Th Stoop, E.A. C Neef, Early stage beneficial effects of cathodic protection in concrete structures, (n.d.). <https://doi.org/10.1002/maco.201005803>.
- [15] S. Teng, T.Y.D. Lim, B. Sabet Divsholi, Durability and mechanical properties of high strength concrete incorporating ultra fine Ground Granulated Blast-furnace Slag, *Constr Build Mater* 40 (2013) 875–881, <https://doi.org/10.1016/j.conbuildmat.2012.11.052>.

- [16] V. Snowlin, H.J. Prabu, A.F. Sahayaraj, I. Johnson, E. Thaninayagam, R.R. Gopi, J. Salamon, A. Simi, Solar assisted removal of methylene blue dye from wastewater using zinc-metal organic framework (Zn-mof), *J. Inorg. Organomet. Polym. Mater.* (2023), <https://doi.org/10.1007/s10904-023-02823-5>.
- [17] A. Felix Sahayaraj, H. Joy Prabu, J. Maniraj, M. Kannan, M. Bharathi, P. Diwahaar, J. Salamon, Metal-organic frameworks (MOFs): the next generation of materials for catalysis, gas storage, and separation, *J. Inorg. Organomet. Polym. Mater.* 33 (2023) 1757–1781, <https://doi.org/10.1007/s10904-023-02657-1>.
- [18] J. Maniraj, F.S. Arockiasamy, C.R. Kumar, D.A. Kumar, I. Jenish, I. Suyambulingam, S.M. Rangappa, S. Siengchin, Machine learning techniques for the design and optimization of polymer composites: a review, *E3S Web of Conferences.* 428 (2023), 02013, <https://doi.org/10.1051/e3sconf/202342802013>.
- [19] A.F. Sahayaraj, S. Dhamotharan, D. Sandeep, P. Ramachandran, I. Jenish, D. Divakaran, I. Suyambulingam, M.R. Sanjay, S. Siengchin, Sustainable smart polymer composite materials: a comprehensive review, *E3S Web of Conferences.* 428 (2023), 02014, <https://doi.org/10.1051/e3sconf/202342802014>.
- [20] J.G. Dai, Y. Akira, F.H. Wittmann, H. Yokota, P. Zhang, Water repellent surface impregnation for extension of service life of reinforced concrete structures in marine environments: the role of cracks, *Cem. Concr. Compos.* 32 (2010) 101–109, <https://doi.org/10.1016/J.CEMCONCOMP.2009.11.001>.
- [21] A. Petcherdchoo, P. Chindaprasirt, Exponentially aging functions coupled with time-dependent chloride transport model for predicting service life of surface-treated concrete in tidal zone, *Cem Concr Res* 120 (2019) 1–12, <https://doi.org/10.1016/J.CEMCONRES.2019.03.009>.
- [22] M.V. Diamanti, A. Brenna, F. Bolzoni, M. Berra, T. Pastore, M. Ormellese, Effect of polymer modified cementitious coatings on water and chloride permeability in concrete, *Constr Build Mater* 49 (2013) 720–728, <https://doi.org/10.1016/J.CONBUILDMAT.2013.08.050>.
- [23] J. De Vries, R.B. Polder, Hydrophobic treatment of concrete, *Constr Build Mater* 11 (1997) 259–265, [https://doi.org/10.1016/S0950-0618\(97\)00046-9](https://doi.org/10.1016/S0950-0618(97)00046-9).
- [24] G. Li, Y. Ding, T. Gao, Y. Qin, Y. Lv, K. Wang, Chloride resistance of concrete containing nanoparticle-modified polymer cementitious coatings, *Constr Build Mater* 299 (2021), 123736, <https://doi.org/10.1016/J.CONBUILDMAT.2021.123736>.
- [25] A. Gupta, C. Srivastava, Correlation between microstructure and corrosion behaviour of SnBi-graphene oxide composite coatings, *Surf. Coat. Technol.* 375 (2019) 573–588, <https://doi.org/10.1016/J.JSURFCOAT.2019.07.060>.
- [26] M. Sánchez, P. Faria, L. Ferrara, E. Horszczaruk, H.M. Jonkers, A. Kwiecień, J. Mosa, A. Peled, A.S. Pereira, D. Snoeck, M. Stefanidou, T. Stryzewska, B. Zajac, External treatments for the preventive repair of existing constructions: a review, *Constr Build Mater* 193 (2018) 435–452, <https://doi.org/10.1016/J.CONBUILDMAT.2018.10.173>.
- [27] A.M. Rashad, A synopsis about the effect of nano-Al<sub>2</sub>O<sub>3</sub>, nano-Fe<sub>2</sub>O<sub>3</sub>, nano-Fe<sub>3</sub>O<sub>4</sub> and nano-clay on some properties of cementitious materials – a short guide for Civil Engineer, *Mater. Des.* 52 (2013) 143–157, <https://doi.org/10.1016/J.MATDES.2013.05.035>.
- [28] R. Bani Ardalan, A. Joshaghani, R.D. Hooton, Workability retention and compressive strength of self-compacting concrete incorporating pumice powder and silica fume, *Constr Build Mater* 134 (2017) 116–122, <https://doi.org/10.1016/J.CONBUILDMAT.2016.12.090>.
- [29] C.K.Y. Leung, M. Asce, H.-G. Zhu, J. Jang-Kyo Kim, R.S.C. Woo, Use of Polymer/Organoclay Nanocomposite Surface Treatment as Water/Ion Barrier for Concrete, (n.d.), <https://doi.org/10.1061/ASCE0899-15612008207484>.
- [30] M. Sánchez, M.C. Alonso, R. González, Preliminary attempt of hardened mortar sealing by colloidal nanosilica migration, *Constr Build Mater* 66 (2014) 306–312, <https://doi.org/10.1016/J.CONBUILDMAT.2014.05.040>.
- [31] G. Fajardo, A. Cruz-López, D. Cruz-Moreno, P. Valdez, G. Torres, R. Zanella, Innovative application of silicon nanoparticles (SN): improvement of the barrier effect in hardened Portland cement-based materials, *Constr Build Mater* 76 (2015) 158–167, <https://doi.org/10.1016/J.CONBUILDMAT.2014.11.054>.
- [32] F. Sandrolini, E. Franzoni, B. Pigino, Ethyl silicate for surface treatment of concrete – Part I: pozzolanic effect of ethyl silicate, *Cem. Concr. Compos.* 34 (2012) 306–312, <https://doi.org/10.1016/J.CEMCONCOMP.2011.12.003>.
- [33] Q. Wang, G.D. Qi, Y. Wang, H.Y. Zheng, S.H. Shan, C.X. Lu, Research progress on the effect of graphene oxide on the properties of cement-based composites, *Xinjing Tan Cailiao/New Carbon Materials* 36 (2021) 729–750, [https://doi.org/10.1016/S1872-5805\(21\)60071-9](https://doi.org/10.1016/S1872-5805(21)60071-9).
- [34] C. Liu, X. Huang, Y.Y. Wu, X. Deng, Z. Zheng, Z. Xu, D. Hui, Advance on the dispersion treatment of graphene oxide and the graphene oxide modified cement-based materials, *Nanotechnol. Rev.* 10 (2021) 34–49, <https://doi.org/10.1515/ntrv-2021-0003>.
- [35] R. Martínez-García, D. González-Campelo, F.J. Fraile-Fernández, A.M. Castañón, P. Caldevilla, S. Giganto, A. Ortiz-Marqués, F. Zelli, V. Calvo, J.M. González-Domínguez, M. Fernández-Raga, Performance study of graphene oxide as an antierosion coating for ornamental and heritage dolostone, *Adv Mater Technol* (2023), <https://doi.org/10.1002/admt.202300486>.
- [36] P.K. Akarsh, D. Shrinidhi, S. Marathe, A.K. Bhat, Graphene oxide as nano-material in developing sustainable concrete – a brief review, *Mater Today Proc* (2022), <https://doi.org/10.1016/J.MATPR.2021.12.510>.
- [37] L. Guadagno, C. Naddeo, M. Raimondo, G. Barra, L. Vertuccio, S. Russo, K. Lafdi, V. Tucci, G. Spinelli, P. Lamberti, Influence of carbon nanoparticles/epoxy matrix interaction on mechanical, electrical and transport properties of structural advanced materials, *Nanotechnology* 28 (2017), 094001, <https://doi.org/10.1088/1361-6528/aa583d>.
- [38] P.P. Brisebois, M. Sijaj, Harvesting graphene oxide-years 1859 to 2019: a review of its structure, synthesis, properties and exfoliation, *J Mater Chem C Mater* 8 (2020) 1517–1547, <https://doi.org/10.1039/C9TC03251G>.
- [39] F. Tardani, W. Neri, C. Zakri, H. Kellay, A. Colin, P. Poulin, Shear rheology control of wrinkles and patterns in graphene oxide films, *Langmuir* 34 (2018) 2996–3002, <https://doi.org/10.1021/acs.langmuir.7b04281>.
- [40] R. Ciriminna, N. Zhang, M.Q. Yang, F. Meneguzzo, Y.J. Xu, M. Pagliaro, Commercialization of graphene-based technologies: a critical insight, *Chem. Commun.* 51 (2015) 7090–7095, <https://doi.org/10.1039/c5cc01411e>.
- [41] A. Habibnejad Korayem, P. Ghoddousi, A.A. Shirzadi Javid, M.A. Oraie, H. Ashegh, Graphene oxide for surface treatment of concrete: a novel method to protect concrete, *Constr Build Mater* 243 (2020), <https://doi.org/10.1016/j.conbuildmat.2020.118229>.
- [42] A. Antolín-Rodríguez, D. Merino-Maldonado, Á. Rodríguez-González, M. Fernández-Raga, J.M. González-Domínguez, A. Juan-Valdés, J. García-González, Statistical study of the effectiveness of surface application of graphene oxide as a coating for concrete protection, *Coatings* 13 (2023) 213, <https://doi.org/10.3390/coatings13010213>.
- [43] EN 197-1. Cement, Part 1: Composition, Specifications and Conformity Criteria for Common Cements, Belgium, Brussels, 2011.
- [44] E.N. Cen, 12620+A1 Aggregates for Concrete, Belgium, Brussels, 2003.
- [45] Cen, EN 933-1 Tests for Geometrical Properties of Aggregates- Part 1: Determination of Particle Size Distribution - Sieving Method, Belgium, Brussels, 2012.
- [46] Structural Code, Royal Decree 470/2021, Spanish Ministry of the Presidency, Relations with the Courts and Democratic Memory, Madrid, 2021.
- [47] D. González-Campelo, M. Fernández-Raga, Á. Gómez-Gutiérrez, I. Guerra-Romero, J.M. González-Domínguez, Extraordinary Protective Efficacy of Graphene Oxide over the Stone-Based Cultural Heritage, 2021, <https://doi.org/10.1002/admi.202101012>.
- [48] L. Hanzic, L. Kosec, I. Anzel, Capillary absorption in concrete and the Lucas–Washburn equation, *Cem. Concr. Compos.* 32 (2010) 84–91, <https://doi.org/10.1016/J.CEMCONCOMP.2009.10.005>.
- [49] Q. Gao, Z. Ma, J. Xiao, F. Li, Effects of Imposed Damage on the Capillary Water Absorption of Recycled Aggregate Concrete, 2018, <https://doi.org/10.1155/2018/2890931>.
- [50] UNE 83982. Durability of Concrete. Test Methods. Determination of Water Absorption by Capillary Action of Hardened Concrete, Fagerlund method., Madrid, Spain, 2008.
- [51] UNE 83966. Durability of Concrete. Test Methods. Conditioning of Concrete Specimens for Gas Permeability and Capillarity Tests, Madrid, Spain, 2008.
- [52] UNE 83980. Durability of Concrete. Test Methods. Determination of Water Absorption, Density and Water Accessible Porosity of Concrete, Madrid, Spain, 2014.
- [53] R. Duarte, I. Flores-Colen, J. de Brito, A. Hawreen, Variability of in-situ testing in wall coating systems - Karsten tube and moisture meter techniques, *J. Build. Eng.* 27 (2020), <https://doi.org/10.1016/j.jobbe.2019.100998>.
- [54] UNE 16302. Conservation of Cultural Heritage. Test Methods. Measurement of Water Absorption by the Pipette Method, Madrid, Spain, 2016.
- [55] UNE 12390-8, Depth of Water Penetration under Pressure, Madrid, Spain, 2020.
- [56] UNE 12390-6, Test on Hardened Concrete. Part 6: Indirect Tensile Strength of Specimens, Madrid, Spain, 2010.
- [57] ImageJ. Computer Software, (n.d.).
- [58] M.R. Hall, D. Allinson, Evaporative drying in stabilised compressed earth materials using unsaturated flow theory, *Build. Environ.* 45 (2010) 509–518, <https://doi.org/10.1016/J.BUILDENV.2009.07.003>.

- [59] H. Zhao, J. Ding, Y. Huang, Yimin Tang, W. Xu, D. Huang, Experimental Analysis on the Relationship between Pore Structure and Capillary Water Absorption Characteristics of Cement-Based Materials, 2019, <https://doi.org/10.1002/suco.201900184>.
- [60] J. Lu, K. Wang, M.L. Qu, Experimental determination on the capillary water absorption coefficient of porous building materials: a comparison between the intermittent and continuous absorption tests, *J. Build. Eng.* 28 (2020), 101091, <https://doi.org/10.1016/J.JOBE.2019.101091>.
- [61] S. Lv, Y. Ma, C. Qiu, T. Sun, J. Liu, Q. Zhou, Effect of graphene oxide nanosheets of microstructure and mechanical properties of cement composites, *Constr Build Mater* 49 (2013) 121–127, <https://doi.org/10.1016/J.CONBUILDMAT.2013.08.022>.
- [62] J.R. Potts, D.R. Dreyer, C.W. Bielawski, R.S. Ruoff, Graphene-based polymer nanocomposites, *Polymer (Guildf)*. 52 (2011) 5–25, <https://doi.org/10.1016/J.POLYMER.2010.11.042>.
- [63] Z. Pan, L. He, L. Qiu, A.H. Korayem, G. Li, J.W. Zhu, F. Collins, D. Li, W.H. Duan, M.C. Wang, Mechanical properties and microstructure of a graphene oxide–cement composite, *Cem. Concr. Compos.* 58 (2015) 140–147, <https://doi.org/10.1016/J.CEMCONCOMP.2015.02.001>.
- [64] UNE 1504-2, Products and Systems for the Protection and Repair of Concrete Structures. Definitions, Requirements, Quality Control and Conformity Assessment. Part 2, Surface protection systems for concrete, Madrid, Spain, 2005.
- [65] Water distribution modelling of capillary absorption in cementitious materials - ScienceDirect, (n.d.). <https://www.sciencedirect.com/science/article/pii/S0950061819311821?via%3Dihub> (accessed June 8, 2023).
- [66] J. Liu, F. Xing, B. Dong, H. Ma, D. Pan, Study on water sorptivity of the surface layer of concrete, *Materials and Structures/Materiaux et Constructions* 47 (2014) 1941–1951, <https://doi.org/10.1617/s11527-013-0162-x>.
- [67] A. Akbar, S. Javid, P. Ghoddousi, Maziar Zareechian, Asghar, H. Korayem, Effects of spraying various nanoparticles at early ages on improving surface characteristics of concrete pavements, *Int. J. Civ. Eng.* 17 (2019) 1455–1468, <https://doi.org/10.1007/s40999-019-00407-4>.
- [68] Y. Zhang, S. Li, W. Zhang, X. Chen, D. Hou, T. Zhao, X. Li, Preparation and mechanism of graphene oxide/isobutyltriethoxysilane composite emulsion and its effects on waterproof performance of concrete, *Constr Build Mater* 208 (2019) 343–349, <https://doi.org/10.1016/J.CONBUILDMAT.2019.03.015>.
- [69] D. Hou, C. Wu, B. Yin, X. Hua, H. Xu, X. Wang, S. Li, Y. Zhou, Z. Jin, W. Xu, H. Lu, Investigation of composite silane emulsion modified by in-situ functionalized graphene oxide for cement-based materials, *Constr Build Mater* 304 (2021), 124662, <https://doi.org/10.1016/J.CONBUILDMAT.2021.124662>.
- [70] P. Scarfato, L. Di Maio, M.L. Fariello, P. Russo, L. Incarnato, Preparation and evaluation of polymer/clay nanocomposite surface treatments for concrete durability enhancement, *Cem. Concr. Compos.* 34 (2012) 297–305, <https://doi.org/10.1016/J.CEMCONCOMP.2011.11.006>.
- [71] G. Li, J. Yue, C. Guo, Y. Ji, Influences of modified nanoparticles on hydrophobicity of concrete with organic film coating, *Constr Build Mater* 169 (2018) 1–7, <https://doi.org/10.1016/J.CONBUILDMAT.2018.02.191>.
- [72] Z. Wang, F. He, J. Guo, S. Peng, X.Q. Cheng, Y. Zhang, E. Drioli, A. Figoli, Y. Li, L. Shao, The stability of a graphene oxide (GO) nanofiltration (NF) membrane in an aqueous environment: progress and challenges, *Mater Adv* 1 (2020) 554–568, <https://doi.org/10.1039/d0ma00191k>.
- [73] B. Yin, C. Wu, D. Hou, S. Li, Z. Jin, M. Wang, X. Wang, Research and application progress of nano-modified coating in improving the durability of cement-based materials, *Prog Org Coat* 161 (2021), 106529, <https://doi.org/10.1016/J.PORGOAT.2021.106529>.
- [74] Z. Pan, L. He, L. Qiu, A.H. Korayem, G. Li, J.W. Zhu, F. Collins, D. Li, W.H. Duan, M.C. Wang, Mechanical properties and microstructure of a graphene oxide–cement composite, *Cem. Concr. Compos.* 58 (2015) 140–147, <https://doi.org/10.1016/J.CEMCONCOMP.2015.02.001>.
- [75] F. Mouhat, F.X. Coudret, M.L. Bocquet, Structure and chemistry of graphene oxide in liquid water from first principles, *Nat. Commun.* 11 (2020), <https://doi.org/10.1038/s41467-020-15381-y>.
- [76] Z. Wang, F. He, J. Guo, S. Peng, X.Q. Cheng, Y. Zhang, E. Drioli, A. Figoli, Y. Li, L. Shao, The stability of a graphene oxide (GO) nanofiltration (NF) membrane in an aqueous environment: progress and challenges, *Mater Adv* 1 (2020) 554–568, <https://doi.org/10.1039/d0ma00191k>.
- [77] J. He, S. Du, Z. Yang, X. Shi, Laboratory investigation of graphene oxide suspension as a surface sealer for cementitious mortars, *Constr Build Mater* 162 (2018) 65–79, <https://doi.org/10.1016/J.CONBUILDMAT.2017.12.022>.